

Raid A. Ismail ¹
Walid K. Hamoudi ²
Yasmeen Z. Daood ³

¹ Physics Science and Research Center, Ministry of Science and Technology, Baghdad, IRAQ.,
raidismail@yahoo.com

² School of Applied Sciences, University of Technology, Baghdad, IRAQ

³ Solar Energy Research Center, Ministry of Industry and Minerals, Baghdad, IRAQ

Band Diagram of p-PbTe/n-Si Heterostructure

In the present work, the energy band diagram of p-PbTe/n-Si heterojunctions made by thermal evaporation of a polycrystalline PbTe layer deposited on a monocrystalline Silicon substrate is constructed. Based on I-V and C-V measurements, the band offsets ΔE_C and ΔE_V are found experimentally to be 270mV and 610mV respectively at 300K.

Keywords: PbTe/Si thin films, Heterojunctions, Energy band diagram

Received: 16 August 2004, Revised: 8 March 2005, Accepted: 15 March 2005

1. Introduction

Heterojunction devices have drawn a great attention in recent years mainly due to their use in the optoelectronic fields [1]. The properties of these heterojunctions are of critical importance when they are used as field-effect transistors (FET), bipolar transistor, light-emitting diode or lasers [2-3].

PbTe on Si structures are used for IR readout and imaging applications [4]. There is some work that has been reported on PbTe/Si heterojunctions where lattice mismatch is quite large. It has been shown that the preparation of the overlay layer plays an important role in the junction quality [5]. Hot-wall epitaxy (HWE) growth is a promising method to grow PbTe; it is clean and mostly reproducible.

Recently we have succeeded in fabricating a good quality PbTe/Si heterojunction using thermal evaporation technique [6]. In this paper, the band line-up of anisotype PbTe/Si heterojunction based on experimental results of I-V and C-V data was constructed. These results are compared with those for PbTe/Si heterojunction prepared by the HWE technique.

2. Experimental Details

Single crystal, 500 μ m thick n-Si wafers with resistivity of (1-3) Ω .cm were used as substrates. They were etched with dilute HF for about 10min in running hot deionized water and then dried. High purity 50 nm thick PbTe was deposited on cold Si substrates using a thermal resistance technique with pressure lower than 10⁻⁷ mbar. X-ray diffraction (XRD) analysis was performed using CuK α radiation to confirm the crystalline structure of the PbTe layer. The

conductivity type and sheet resistance of the PbTe films were investigated using Hall and four point probe measurements respectively.

Ohmic contacts were made on both, PbTe and Si, by deposition of In and Al, respectively. After contacts and assembly processes I-V (with different operating techniques) and C-V (10kHz) characteristics of the heterojunctions were investigated.

3. Results and Discussion

Fig. (1) shows an XRD spectrum of the PbTe films without post-deposition annealing. It is clear that the film is polycrystalline. Four peaks are observed in the pattern and can be indexed to the structure of PbTe with lattice constant of 0.645 nm. No diffraction peak corresponding to elements of Pb and Te were detected in any of our samples. Hall measurements confirm that PbTe and hence an anisotype heterojunction was formed.

A C-V characteristics of the heterojunction is shown in Fig. (2). It shows a straight line (abrupt junction) plot where 1/C²=0 points to the value of the built-in-voltage (V_D) according to the equation [7]:

$$V_D = V_{int} + \frac{2KT}{q} \quad (1)$$

was calculated to be 0.6V. This is higher than the theoretical value, possibly due to the large degree of lattice mismatch (18%).

Fig. (3) depicts the dark I-V curve of the heterojunction at 300K. By applying the equation [3]:

$$n = \frac{KT}{q} \cdot \frac{\Delta V}{\ln \frac{I_p}{I_s}} \quad (2)$$

where KT/q is thermal voltage, I_s saturation current, the ideality factor (n) was deduced by Eq.(2) to be 1.6. This shows a mixed generation-recombination and diffusion current [8].

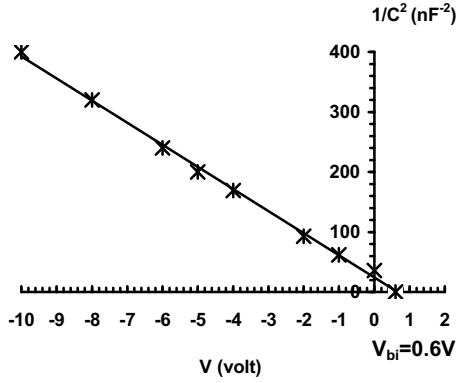


Fig. (2) $1/C^2$ with reverse bias voltage

Fig. (4) shows the semi-log scale of the temperature dependent I-V curves of the heterojunction. At lower temperature $<298K$ no measurable current was noticed due to the

exponential decrease of the current concentration at lower temperatures. From the I-V-T curves, the saturation currents were calculated and plotted as a function of $(1/T)$ (Fig. 5).

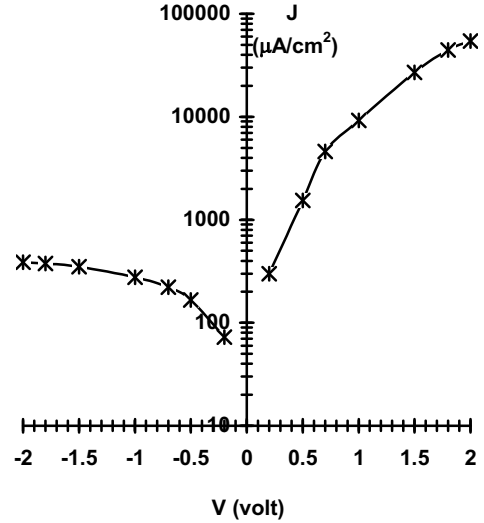


Fig. (3) Current-voltage characteristics for p-PbTe/n-Si anisotype heterojunction

The value of valence band offset ΔE_V was deduced from the slope of Fig. (5) using the

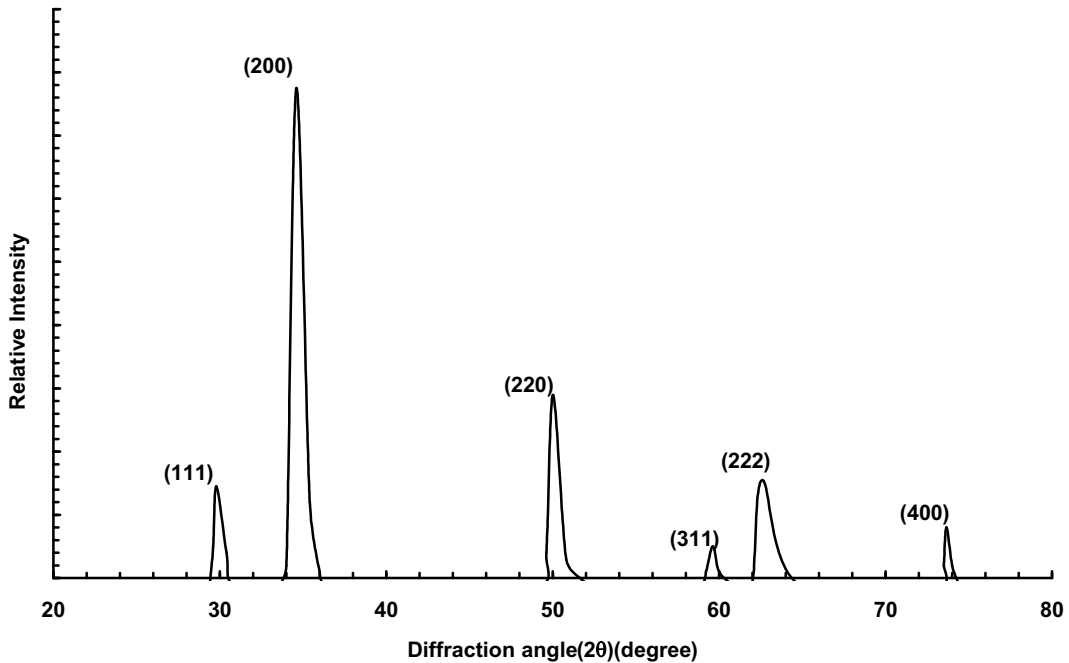


Fig. (1) X-ray diffraction spectrum of PbTe films

following equation [9,10]:

$$J_s = A \exp\left[\frac{-q(V_D - \Delta E_V)}{KT}\right] \quad (3)$$

ΔE_V was found to be 610meV where A is constant.

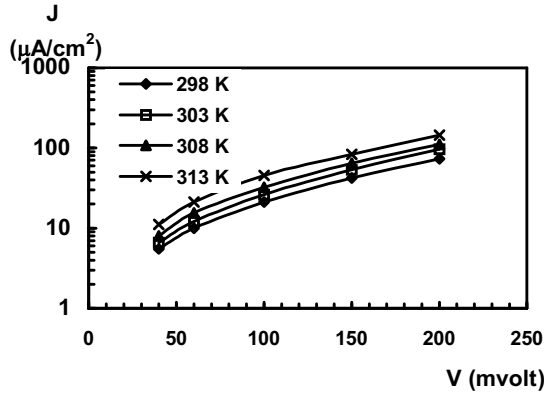


Fig. (4) Forward current density (J) against voltage (V) at temperatures between 298K and 313K

After inserting the band gap values for PbTe (0.30 eV) and for Si (1.11 eV), ΔE_C was calculated to be around 210meV. These values of band offset are slightly different from those reported by Vaya *et al.* [11]. This is attributed to the role of the preparation method of the PbTe layer. Fermi levels in PbTe (E_{fp}) and in Si (E_{fn})

were calculated and hence the energy band diagram was constructed and presented in Fig. (6). It is obvious from the band diagram that the band bending occurs only on the wide band gap (Si) while the bands remain flat in the PbTe side. This result is in good agreement with the result obtained by Vaya *et al.*

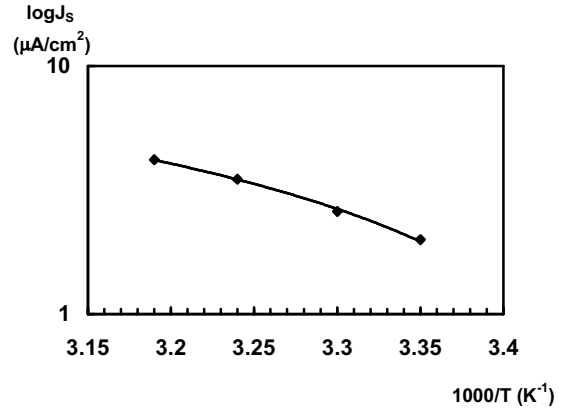


Fig. (5) J_s versus $1000/T$ for determination ΔE_V

The value of the conduction band offset ΔE_C was determined using the formula [8]:

$$\Delta E_C = E_g(\text{Si}) - E_g(\text{PbTe}) - \Delta E_V \quad (4)$$

4. Conclusions

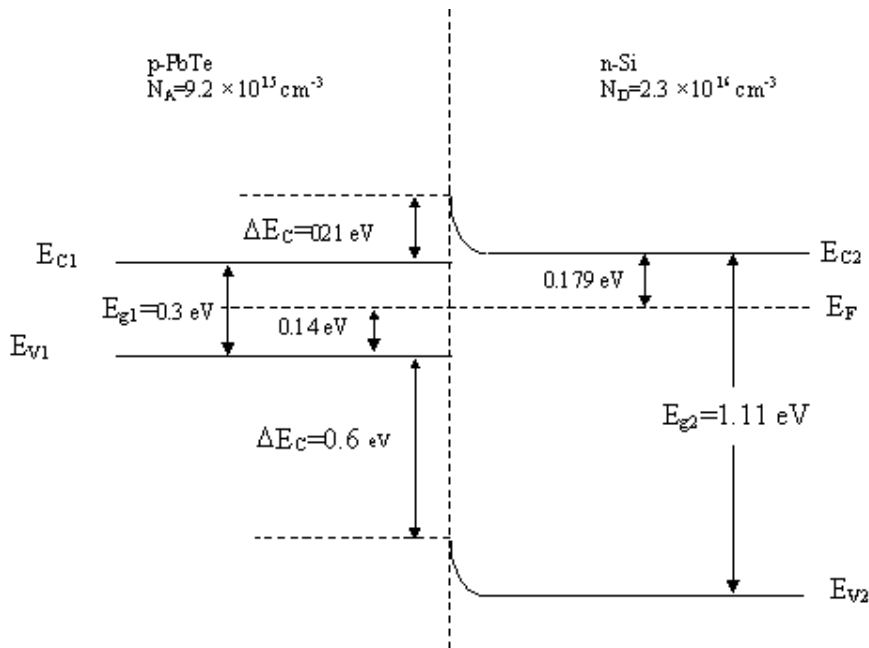


Fig. (6) Energy band diagram for p-PbTe/Si heterojunction

The band line-up of anisotype PbTe/Si heterojunction was constructed with the aid of I-V and C-V characteristics at 300K. The band diagram shows that despite the high resistivity of the deposited PbTe layer the PbTe/Si heterojunction behaves like a simple Schottky barrier device.

References

- [1] R.A. Ismail and M.S. Mohammad, *J. Eng. Tech.* (Iraq), Vol.19 (2000).
- [2] S.M. Potrous, *J. Eng. Tech.*, Vol.15(6) (1996), pp. 40-43.
- [3] Zh.I. Alferov, “**Semiconductor Heterostructures: Physical Processes and Applications**”, MIR Publishers (Moscow), (1989).
- [4] K. Alchalabi, D. Zimin and H. Zogg, *IEEE Electron. Device Lett.*, Vol.3 (2001), pp.110-112.
- [5] D.A. Neamen, “**Semiconductor physics and Devices**”, McGraw-Hill (New York), (1992).
- [6] W.K. Hamoudi, R.A. Ismail and Y.Z. Daood, *J. Eng Tech.* (Iraq), Vol.23(5) (2004), pp. 236-245.
- [7] B. Sapoval and C. Hermann, “**Physics of Semiconductors**”, Springer-Verlag (New York) (1995).
- [8] S. Fujita, T. Yodo and A. Sasaki, *J. Cryst. Growth*, Vol.72 (1985), pp. 27-30.
- [9] P.R. Vaya, J. Majhi, B.S.V. Gopalam and C. Dattatreynan, *Phys. Stat. Sol. (a)*, Vol.93(1) (1986), pp. 355-360.
- [10] A. Georgakilas, E. Aperathitis, V. Foukaraki, M. Kayambaki and P. Panayotatos, *Mater. Sci. Eng.*, Vol.B44 (1997), pp. 383-386.
- [11] V. D. Das and K. S. Bhat, *J. Appl. Phys.*, Vol.22 (1989), pp.126-168.
-
-